Spectrochimica Acta Part A: Molecular and Biomolecular Spectroscopy 223 (2019) 117342

Contents lists available at ScienceDirect

Spectrochimica Acta Part A: Molecular and Biomolecular Spectroscopy

journal homepage: www.elsevier.com/locate/saa

Structural and spectroscopic properties of Er^{3+} doped sodium lithium borate glasses

Juniastel Rajagukguk [a,*], Fitrilawati [b], Bornok Sinaga [c], Jakrapong Kaewkhao [d]

[a] Department of Physics, Faculty of Mathematics and Natural Sciences, Universitas Negeri Medan, 20221, Indonesia
[b] Department of Physics, Faculty of Mathematics and Natural Sciences, Universitas Padjadjaran, 45363, Indonesia
[c] Faculty of Mathematics and Natural Sciences, Universitas Negeri Medan, 20221, Indonesia
[d] Center of Excellence in Glass Technology and Materials Science, Nakhon Pathom Rajabhat University, Nakhon Pathom 73000, Thailand

ARTICLE INFO

Article history:
Received 17 October 2018
Received in revised form 10 June 2019
Accepted 7 July 2019
Available online 09 July 2019

Keywords:
Erbium
Borate glass
Judd-Ofelt parameters
Radiative properties
Emission cross section

ABSTRACT

The trivalent erbium (Er^{3+}) doped sodium lithium borate glass with composition (65-x)B_2O_3-15Na_2O-10PbO-5ZnO-5Li_2O-xEr_2O_3 have been successfully fabricated by melt-quench technique. The structural properties were investigated by X-ray diffraction (XRD) and Fourier Transform Infrared (FTIR). The absorption and luminescence spectra of glass samples were measured to determine the spectroscopic properties. The Judd–Ofelt parameters were calculated based on absorption spectra with values of Ω_2, = 4.39, Ω_4 = 3.22, and Ω_6 = 0.91 ($\times 10^{-22}$ cm^2) for 2.0 mol% Er^{3+} ion doped sodium lithium borate glass. Furthermore, radiative properties including effective bandwidth ($\Delta\lambda_{eff}$), radiative transition probability (A_R), radiative lifetime (τ_R), and branching ratio (β_R) were also calculated and analyzed. A strong emission band at 1532 nm was observed corresponding to $^4I_{15/2} \rightarrow {}^4I_{13/2}$ transition under the excitation wavelength of 528 and 976 nm. The stimulated emission cross-section (σ_e) and figure of merit (FWHM xσ_e) were calculated and compared with other glasses in order to evaluate the properties of the present samples for optical amplifier. Based on the characterization results, we found that the glass with 2.0 mol% Er^{3+} ion doped sodium lithium borate glass had the highest stimulated emission cross section compared to other samples and were comparable with the previous reports.

1. Introduction

In last few decades, trivalent lanthanide (Ln^{3+}) ions doped glasses former have been widely studied due to their importance in several applications such as telecommunication, solid-state laser, optical sensors, and optical amplifier [1,2]. Numerous publications have reported lanthanide group doped borate-based glass such as Europium (Eu^{3+}) [3], Neodymium (Nd^{3+}) [4], Samarium (Sm^{3+}) [5], Dysprosium (Dy^{3+}) [6], and Erbium (Er^{3+}) [7]. Among those various Ln^{3+} ions group, Er^{3+} ions doped borate glass containing other modifiers is one of most interesting work for laser application [8]. Moreover, Er^{3+} ions doped glasses also have a great potential to be used as optical amplifier due to strong emission band from $^4I_{13/2} \rightarrow {}^4I_{15/2}$ transition. In addition, a wide range of wavelength at infrared region about 1350–1650 nm also makes it a good candidate for laser infrared.

Glass former based on borate (B_2O_3) is one of the excellent glass former and the most famous one. It has outstanding properties such as high transparency, high chemical durability, good thermal stability, homogeneity, easy to prepare, and relatively low melting point [9–12]. The homogeneous mixture of dopant ions in the glass former usually can be enhanced by adding another constituent so-called network modifiers. There are several network modifiers that had been used such as sodium oxide (Na_2O), aluminum oxide (Al_2O_3), lead oxide (PbO), zinc oxide (ZnO), bismuth oxide (Bi_2O_3) and lithium oxide (Li_2O) [13]. The addition of those metal oxide modifiers to the glass former could affect the fundamental network of its glass. This also could lead to improve the stability, inhibit the moisture and lower the temperature process [14]. For example, lithium oxide, can strengthen the structural bonding through the formation of ionic bonds with oxygen (non-bridging oxygen) and is able to reduce the basic hygroscopic of borate glass. Sodium oxide (Na_2O) has a role to expand the homogenization and decrease the melting point. On the other side, ZnO can enhance the optical and structural properties when it is mixed into a glass former. It is also well known that PbO acts as network former and is capable to increase the glass conductivity. Therefore, the optimum properties a glass can be achieved by mixing several network modifiers with a proper composition. Several researchers have reported their works on Ln^{3+} ion doped borate glasses such as Er^{3+} doped lithium zinc borate [15], 60Bi_2O_3–20B_2O_3–(20–x)Ga_2O_3–xEr_2O_3 [16], Dy^{3+}/Sm^{3+} doped 44.5ZnO–15PbO–40B_2O_3 [17], and 27Li_2O- 3Al_2O_3–(70-X)B_2O_3-X Dy_2O_3 [18]. They considered that those glass systems can be used for high energy solid state laser, light source for heavy bluish yellow color, highly luminescent Opt. Mater. and suitable for White-LED.

* Corresponding author.
E-mail address: juniastel@unimed.ac.id (J. Rajagukguk).

https://doi.org/10.1016/j.saa.2019.117342
1386-1425/

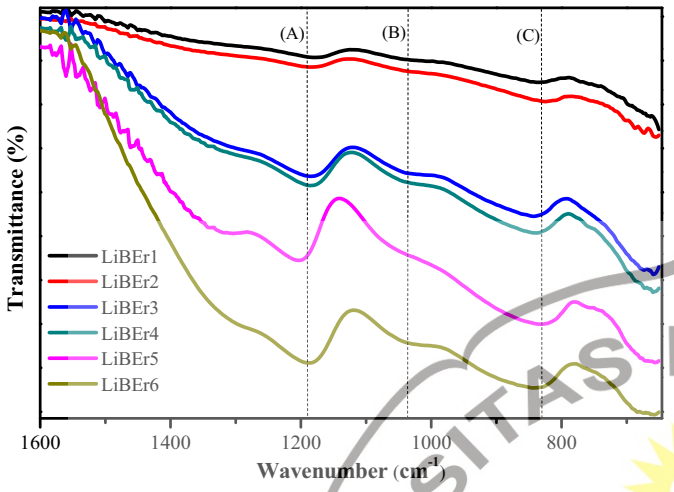

Fig. 1. Infrared spectra of Er^{3+} doped sodium lithium borate glasses system.

In this present work, we study structural and spectroscopic properties of Er^{3+} doped borate glasses containing several modifiers such as Na_2O, PbO, ZnO and Li_2O with different Er^{3+} ion concentrations. The structural properties were investigated by X-ray diffraction (XRD) and Fourier Transform Infrared (FTIR). The absorption and luminescence spectra of glass samples were measured to determine the spectroscopic properties. The Judd–Ofelt parameter was calculated based on absorption spectra. Furthermore, radiative properties including effective bandwidth ($\Delta\lambda_{eff}$), radiative transition probability (A_R), radiative life time (τ_R), and branching ratio (β_R) were also calculated and analyzed. We found that Er^{3+} ion doped sodium lithium borate glass significantly enhanced optical absorption, luminesce emission spectra and spectroscopic properties.

2. Experimental

All the raw powder materials of B_2O_3 (99.99%, Ajax Finechem Pty Ltd), Na_2O (99.95%, Sigma-Aldrich), PbO (99.7%, Acros Organics), ZnO (99.99%, Acros Organics), Li_2O (99.99%, Acros Organics) and Er_2O_3 (99.99%, Sigma-Aldrich) with analytical grade) were directly used without any treatment.

Er^{3+} ion doped sodium lithium borate glass was prepared based on chemical composition:

$$(65-x)B_2O_3-15Na_2O-10PbO-5ZnO-5Li_2O-xEr_2O_3$$

where x = 0, 0.05, 0.1, 0.5, 1.0, 2.0 and 4.0 mol%, and denoted as LiBEr, LiBEr1, LiBEr2, LiBEr3, LiBEr4, LiBEr5, and LiBEr6, respectively. The glass samples were fabricated by the conventional melt-quench method, as follows. 20 g of raw materials were mixed to obtain the homogeneous compound and placed to alumina crucible. Then, the alumina crucible was transferred to an electric furnace and heated at 1100 °C for 4 h. Subsequently, the melts were poured into a stainless steel plate to obtain a shape. After that, the glass was annealed at 350 °C for 3 h in another electric furnace. Finally, after cooling down to room temperature, the as-prepared sample was cut and polished before being used for measurements.

X-ray diffraction (XRD) patterns were recorded by LabX XRD-6100 (Shimadzu). A Cary 630 Fourier Transform Infrared (FTIR) spectrometer was performed to study the structural properties of samples. The absorption spectra were recorded at a range of 300–1700 nm by UV–Vis-NIR spectrophotometer (UV-3600 Shimadzu). Based upon absorption spectra, the optical band gap energy (E_{opt}) of the sample was calculated by Tauc's plots. The fluorescence spectra in the near-infrared region were evaluated by using PTI Quanta Master series (QM-300) spectrofluorometer with a pulsed xenon lamp as the light source. To further study the spectroscopic properties, the Judd-Ofelt intensity parameter was conducted. The radiative properties of samples were obtained by theoretical calculation.

3. Results and discussion

3.1. Structural analysis

To study the structural properties of glass samples, Fourier-Transform Infrared (FTIR) spectra were performed at range wavenumber of 600 to 1600 cm^{-1}, as shown in Fig. 1. It is clearly observed that there is a slight difference of peak position between un-doped and doped with Er^{3+}. However, after doping with more Er^{3+} concentration (beyond 0.05% mol) all peaks appear more clearly compared to un-doped (LiBEr1). The peak absorption bands related to vibration modes of Er^{3+} doped sodium lithium borate glasses are summarized in Table 1. The FTIR spectrum of the glass sample consists of three main vibration band which is consistent to borate network in the previous studies [19,20]. Those vibration band are located at wavenumber range 1178–1202 cm^{-1} (A), 1042–1052 cm^{-1}(B) and 823–842 cm^{-1} (C). Each vibration band can be explained as follows. The first vibration band at wavenumber of 1178–1202 cm^{-1} region is assigned as asymmetric stretching of the B—O vibrations in triangular BO_3 unit as has been widely suggested by many authors [20,21]. The second vibration band located at 1042–1052 cm^{-1} region is attributed from the presence of B—O bond stretching of tetrahedral BO_4 units [22]. Lastly, vibration band at 823–842 cm^{-1} region indicates the bending vibration B—O—B of various borate groups [23]. This band also known as the oxygen bridges between one tetragonal unit and one trigonal boron atom. X-ray diffractometer was performed to further study the structural properties of Er^{3+} ion doped sodium lithium borate glass. Fig. 2 exhibits X-ray diffraction patterns of Er^{3+} doped sodium lithium borate glasses with different Er^{3+} ions concentrations. All samples have the similar shape and broad diffraction peaks at 27° and 44°. Those broad peaks indicate that all samples are amorphous nature and do not have any crystalline phase.

3.2. UV–Vis-NIR absorption spectra

The optical absorption spectra of undoped and Er^{3+} ion doped sodium lithium borate glasses were evaluated at UV–Vis-NIR region. Fig. 3 depicts optical absorption spectra of undoped and Er^{3+} doped borate glasses at UV–Vis-NIR region. It can be clearly seen that several peaks absorption band appear at 365, 380, 407, 451, 489, 521, 543, 652, 797, 974 and 1528 nm. Those peaks correspond to energy transition from the ground state $^4I_{15/2}$ to the higher energy states of $^4G_{9/2}$, $^4G_{11/2}$, $^2H_{9/2}$, $^4F_{5/2}$, $^4F_{7/2}$, $^2H_{11/2}$, $^4S_{3/2}$, $^4F_{9/2}$, $^4I_{9/2}$, $^4I_{11/2}$ and $^4I_{13/2}$, respectively. There are three absorptions at near-infrared (NIR) wavelength with the wavelength of 797, 974 and 1528 nm. However, the highest

Table 1
Peak positions and FTIR assignments of Er^{3+} doped sodium lithium borate glass.

Peak	LiBEr1 (cm^{-1})	LiBEr2 (cm^{-1})	LiBEr3 (cm^{-1})	LiBEr4 (cm^{-1})	LiBEr5 (cm^{-1})	LiBEr6 (cm^{-1})	Assignments
A	1178	1181	1185	1185	1202	1185	Asymmetric stretching of the B—O vibrations in triangular BO_3 units
B	1030	1030	1042	1046	1052	1030	B—O bond stretching of tetrahedral BO_4 units
C	835	823	842	838	833	835	Bending vibration of B—O—B in various borate groups

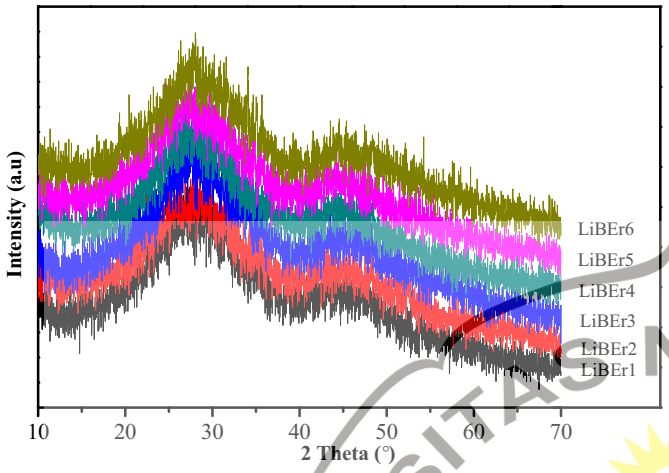

Fig. 2. X-ray diffraction pattern of Er^{3+} doped sodium lithium borate glasses system.

optical absorption is found at band transition from $^4I_{15/2} \rightarrow {}^2H_{11/2}$ with a wavelength of 1528 nm. Fig. 3 also exhibits that the addition of Er_2O_3 to lithium borate glass significantly increases absorption at UV–Vis-NIR region.

One of the important properties to study the effect of absorption is optical band gap energy (E_g). In this regard, absorption edge is very helpful to investigate the optical transitions and electronic band structure of a material [24]. Therefore, to calculate the optical band gap energy (E_g), the Tauc's plot was conducted as shown in Fig. 4 and Fig. 5 for direct and indirect band gap energy, respectively. The linear extrapolation results of direct and indirect of Er^{3+} ion doped sodium lithium borate glass are summarized in Table 2. It can be seen that the band gap value for direct transition slightly decreases from 3.800 to 3.735 eV for LiBEr (undoped Er^{3+}) to LiBEr1 (0.05 mol%Er^{3+}). However, further increasing the Er^{3+} concentration from LiBEr1 to LiBEr6 samples, the direct band gap energies also increase from 3.735 to 3.824 eV. In the same trend also occurs for indirect band gap, the E_g value for undoped Er^{3+} (3.186 eV) is slightly higher than LiBEr1 (0.05 mol% Er^{3+}) with band gap of 3.049 eV. Whereas for LiBEr1 to LiBEr5 samples, the indirect E_g relative increases with increasing Er^{3+} ion concentration. However, the band gap of LiBEr6 slightly decreases by 0.012 eV with the addition of Er^{3+} concentration from 2.0 mol% to 4.0 mol%. These conditions related to change in glass compositions and structure in the local environment configuration of the glass former [25].

3.3. Spectral intensities and intensity parameters

The experimental oscillator strength (f_{exp}) and calculation oscillator strengths (f_{cal}) can be determined by using Eq. (1) and Eq. (2) [26], respectively:

$$f_{exp} = 4.318 \times 10^{-9} \int \varepsilon(\nu) d\nu \quad (1)$$

$$f_{cal}(\Psi J, \Psi' J') = \frac{8\pi^2 mc}{3h} \frac{\bar{\nu} E (n^2+2)^2}{9n(2J+1)} \sum_{\lambda=2,4,6} \Omega_\lambda \left| \langle \Psi J | U^\lambda | \Psi' J' \rangle \right|^2 \quad (2)$$

Table 3 provides both of calculated and experimental oscillator strength (f_{cal} and f_{exp}) for absorption transition of LiBEr3, LiBEr4, LiBEr5 and LiBEr6. We found that transition $^4I_{15/2} \rightarrow {}^4G_{11/2}$ and $^4I_{15/2} \rightarrow {}^2H_{11/2}$ with wavelength of 380 and 521 nm, respectively, have the highest absorption compared with other transitions. The oscillator strength for those transitions as shown in Table 3 also prove to be the highest values compared with other transitions. The transitions $^4I_{15/2} \rightarrow {}^4G_{11/2}$ and $^4I_{15/2} \rightarrow {}^2H_{11/2}$ can be called hypersensitive transitions because of changes in the local structure of the glass network. The hypersensitive transition obeys the quadric-pole selection rules $|\Delta L| \leq 2$, $|\Delta J| \leq 2$ and $\Delta S = 0$ [27,28] that expresses the interaction strength of Er^{3+} dopant ion with host glass in the local structure. It can be seen clearly from Table 3 that both calculated and experimental oscillator strength values significantly decrease with increasing the Er^{3+} ion concentration. The highest calculated and experimental oscillator strength at band transition $^4I_{15/2} \rightarrow {}^4G_{11/2}$ are 32.17×10^{-6} and 33.76×10^{-6} for LiBEr3 sample. The root means square deviation ($\delta_{rms} \times 10^{-6}$) was also conducted to validate the spectrum intensity quality by fitting experimental and calculated oscillator strengths. The reliable calculation is indicated by the small rms deviations value. The maximum and minimum rms deviations are 1.82×10^{-6} and 0.753×10^{-6} for LiBEr3 and LiBEr6, respectively. Overall, the rms deviation values of LiBEr3, LiBEr4, LiBEr5 and LiBEr6 are in the agreement limit.

The Judd-Ofelt intensity parameter ($\Omega_{2,4,6}$) was calculated based on Eq. (3) [26] through the least-square fitting method to understand the local structure of Er^{3+} doped sodium lithium borate glasses. The values $\Omega_{2,4,6}$ of LiBEr3, LiBEr4, LiBEr5 and LiBEr6 together with several other

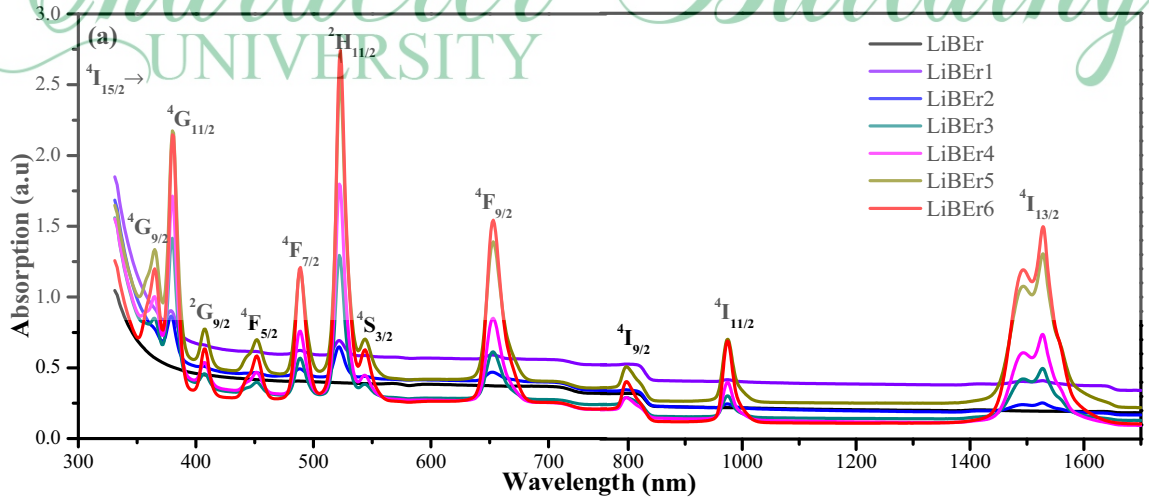

Fig. 3. Optical absorption spectra of Er^{3+} doped sodium lithium borate glasses system at UV–Vis-NIR range.

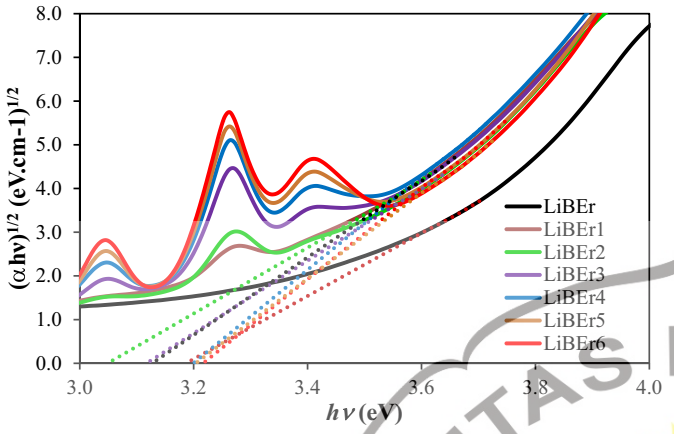

Fig. 4. Tauc's plot for indirect band gap energy of Er^{3+} ion doped sodium lithium borate glasses.

similar glasses containing Er^{3+} ions are listed in Table 4. The three intensity parameters for LiBEr3, LiBEr4 and LiBEr5 samples follow the trend $\Omega_2 > \Omega_4 > \Omega_6$, which are similar trend to Er^{3+} doped BSGdCa glass [29], Er^{3+} doped lithium-borate glass [30], Er^{3+} doped PB glass and Er^{3+} doped PB8 [31]. Whereas for LiBEr6 sample has a different trend as following $\Omega_4 > \Omega_2 > \Omega_6$ and is similar to reported glass in the literature [32]. From Table 4 also can be observed the maximum parameter of 8.72×10^{-20} cm^2 and the minimum of 0.013×10^{-20} cm^2 corresponding to Ω_2 and Ω_6 intensity parameters, respectively, for LiBEr3 sample. Generally, the Ω_2 parameter is associated to the asymmetry of Er^{3+} ion and covalent bonding between Er^{3+} ions with the local environment ligands of the host matrix glass. We observe that with increasing the Er^{3+} ion concentrations from the 0.5 to 4 mol% lead to decrease Ω_2 value from 8.72×10^{-20} to 0.96×10^{-20} cm^2. It is worth noting that N. Vijaya et al. [33] stated that samples with higher intensity parameters of Ω_2 and Ω_4 but lower Ω_6 can be considered as the good host glass. Host glass with the highly covalent bond of Er^{3+} ion and local environment ligand have high luminescence intensity ratio [34]. The Ω_4 and Ω_6 JO intensity are long-range variables, usually the value of Ω_6 parameter related to the rigidity of host matrix. The Ω_6 parameter values increase from 0.013×10^{-20} to 0.91×10^{-20} cm^2 by increasing the Er^{3+} concentrations from the 0.5 to 4 mol%. It indicates that LiBEr6 has higher rigidity compared to other samples. While the Ω_4 JO intensity is the

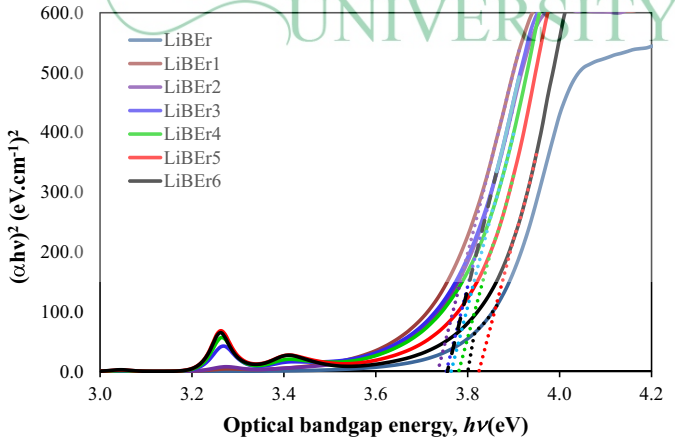

Fig. 5. Tauc's plot for direct band gap energy of Er^{3+}doped sodium lithium Borat glasses doped.

Table 2
Direct and indirect optical band gap energy.

Samples	Direct Eg (eV)	Indirect Eg (eV)
LiBEr_0	3.800	3.186
LiBEr_1	3.735	3.049
LiBEr_2	3.753	3.117
LiBEr_3	3.756	3.127
LiBEr_4	3.764	3.199
LiBEr_5	3.780	3.216
LiBEr_6	3.824	3.204

moderate parameter which depends on Ω_6 and Ω_2 [35].

$$\Omega_\lambda = (2\lambda + 1) \sum_t \sum_p \frac{|A_{t,p}|^2}{2t+1} \Xi^2(t,\lambda) \quad (3)$$

3.4. NIR emission spectra

The near-infrared luminescence of Er^{3+} ion doped sodium lithium borate glasses system was observed under excitation wavelength of 528 nm and 975 nm. Fig. 6 shows the emission of Er^{3+} ion doped lithium borate glass by excitation wavelength of 582 nm. The luminescence spectra located at 1532 nm corresponding to $^4F_{13/2} \rightarrow {}^4I_{15/2}$ transition. The NIR luminescence spectra were recorded by an excitation wavelength of 976 nm and shown in Fig. 7. The emission peak of LiBEr4 glass located at 1525 nm which is slightly shifted to the lower wavelength. However, for other glasses, the emission is found at 1542 nm with shifting to a higher wavelength. The luminescence intensity is observed increasing with the addition of Er^{3+} ion concentration from 0.05 to 1.0 mol%. Further increasing Er^{3+} ion concentration >1.0 mol% the luminescence spectra gradually decreases. The highest emission intensity was found for sample 1 mol% both under the excitation wavelength of 582 and 975 nm. The reason for different peak profile and intensity of LiBEr glass is related to the local ligand fields around Er^{3+} sites [16]. By doping Er^{3+} with different concentration into borate host glass, the content of borate (B_2O_3) decreases which causes the changing of local ligand field near the Er^{3+} sites. The similar phenomenon was also reported in the previous study [36]. The other possible factor is due to effect of radiation trapping [37].

Generally, the $^4I_{15/2} \rightarrow {}^4I_{13/2}$ transition has the broader bandwidth, defined as $\Delta\lambda_{eff}$ and associate to the electric and magnetic dipoles by $S_{ed}/(S_{ed} + S_{md})$ value [38]. The measured luminescence spectra of the Er^{3+} doped sodium lithium borate glasses were used to determine spectroscopic parameters such as effective bandwidth ($\Delta\lambda_{eff}$), radiative transition probability (A_R), and stimulated emission cross section (σ_e). The stimulated emission cross-section for NIR region of Er^{3+} doped sodium lithium borate glass is evaluated by using below equation:

$$\sigma_e = \frac{\lambda_p^4}{8\pi c n^2 \Delta\lambda_{eff}} A_R[\psi J, \psi' J'] \quad (4)$$

where λ_p is the emission peak wavelength, $A_R[\Psi J, \Psi' J']$ is radiative transition probability respectively and $\Delta\lambda_{eff}$ is effective luminescence linewidth which can be obtained through formula [39]:

$$\Delta\lambda_{eff} = \frac{\int I(\lambda) d\lambda}{\bar{I}} \quad (5)$$

where $\bar{I}$ is the average intensity of the integrated area.

Table 5 lists the radiative properties including emission emission peak wavelength (λ_p), effective bandwidth ($\Delta\lambda_{eff}$), emission cross-section ($\sigma_e(\lambda_p)$, branching ratio (β_R), lifetime (τ_R), radiative transition probability (A_R) and FOM (FWHM × σ_e) of Er^{3+} ion doped sodium

Table 3
Experimental (f_{exp}) and theoretical (f_{cal}) oscillator strength values ($\times 10^{-6}$) for various Er^{3+}-doped sodium lithium borate glass systems.

Transitions	λ_{abs} (nm)	Energy (cm^{-1})	LiBEr3		LiBEr4		LiBEr5		LiBEr6	
$^4I_{15/2}\rightarrow$			f_{exp}	f_{cal}	f_{exp}	f_{cal}	f_{exp}	f_{cal}	f_{exp}	f_{cal}
$^4G_{9/2}$	365	27,397.26	4.48	6.66	3.88	5.67	2.98	2.43	3.44	3.45
$^4G_{11/2}$	380	26,315.79	32.17	33.76	25.48	26.49	15.18	15.30	9.39	9.49
$^2H_{9/2}$	407	24,570.02	2.31	0.47	2.48	0.47	1.75	0.65	1.39	0.25
$^4F_{5/2}$	451	22,172.95	3.35	0.01	3.38	0.06	1.81	0.44	1.69	0.01
$^4F_{7/2}$	489	20,449.90	6.34	3.04	5.46	2.72	3.23	2.12	2.85	1.58
$^2H_{11/2}$	521	19,193.86	20.72	19.19	16.05	15.06	8.75	8.68	5.52	5.41
$^4S_{3/2}$	543	18,416.21	0.71	0.01	0.83	0.05	0.31	0.36	0.50	0.01
$^4F_{9/2}$	652	15,337.42	8.32	8.27	7.26	7.07	3.06	3.27	4.16	4.27
$^4I_{9/2}$	797	12,547.05	2.54	2.19	1.84	1.85	0.95	0.70	1.17	1.13
$^4I_{11/2}$	974	10,266.94	0.60	0.25	0.51	0.23	1.73	0.49	0.32	0.03
$^4I_{13/2}$	1528	6544.50	0.13	0.89	0.15	0.85	0.69	1.14	0.06	0.42
rms deviation			±1.820		±1.623		±0.766		±0.753	

lithium borate glass together with comparison data from other reports. From Table 5 can be seen that effective bandwidth properties significantly increase from 91.12 to 98.36 for sample LiBEr3 to LiBEr4. The slight increasement of 1.6 nm is observed for sample LiBEr5 compared to LiBEr4. However, the effective bandwidth of LiBEr6 with a value of 100.34 nm is close to that LiBEr5. The effective bandwidth of this present work is much higher than several previous studies as listed also in the Table 5.

The full width at half maximum (FWHM) is an important property to know the possibility of optical channels in enhancing signal for wavelength-division multiplexing (WDM) systems [40]. In Table 5, we observe that the FWHM values increase from 97.79 nm to 104.86 nm when Er^{3+} ion concentrations increase from 0.5 to 2.0 mol%. However, further increasing the Er^{3+} ions concentration to 4 mol% the FWHM decrease to 95.64 nm. Those FWHM values are higher than other Er^{3+} doped lead zinc borate (Er^{3+}-2PbO·4ZnO·$5B_2O_3$) [41]. The FWHM and effective bandwidth broadness with the addition of Er^{3+} ion concentration might be caused by two main factors. First is a modify of glass structure after doping with Er^{3+} leads to decreasing the B_2O_3 content which results of enhancing inhomogeneous broadening [42]. To support this statement, Xu et al. [43] reported that the FWHM broadness proportional to the line strength of electric dipole transition (S_{ed}). The value of S_{ed} for $^4I_{13/2} \rightarrow {}^4I_{15/2}$ transition according to equation in ref. [44] strongly depends on Ω_6 intensity parameter as the most dominant factor and it can be increased by modifying the glass structure. They found that higher Ω_6 had the wider FWHM. Similarly, this present glass sample with higher Ω_6 value (see Table 3) provides the wider FWHM and effective bandwidth. Second factor is enhancement of covalent bonding of Er—O. After increasing the Er^{3+} ion concentration, the covalent bonding between ions Er—O also increases as have been confirmed previously by Ω_2 parameter in Table 3. It indicates an enhancement of the crystal field of the O^{2-} ligands around the Er^{3+} site, which changes energy level of the Er^{3+} and strengthen the Stark splitting of the $^4I_{13/2} \rightarrow {}^4I_{15/2}$ transition [45].

Table 4
Judd-Ofelt intensity parameters ($\times 10^{-20}$ cm^2) for various Er^{3+} doped sodium lithium borate glasses.

Samples	Ω_2	Ω_4	Ω_6	Ref.
LiBEr3	8.72	7.69	0.013	This work
LiBEr4	6.19	5.68	0.13	This work
LiBEr5	4.39	3.22	0.91	This work
LiBEr6	0.96	5.29	0.014	This work
BSGdCaEr05	3.16	1.32	0.99	[29]
Lithium-borate	3.24	0.92	0.82	[30]
PB8	8.65	1.88	1.15	[31]
BLNEr	3.358	1.342	0.789	[32]

The stimulated emission cross-section (σ_e) is also considered as one of the important factors for optical amplifier application, the larger of its value represents the low threshold and high gain laser operation. The value of 3.96×10^{-21} is highest emission cross section in this work which is obtained by LiBEr5 sample with 2 mol% Er^{3+} ion concentration. This value is slightly higher compared to 3.22×10^{-21} of Er^{3+} doped borate-based tellurium calcium zinc niobium oxide (TCZNBEr1) [46]. The changes stimulated emission cross section of Er^{3+} doped lithium-borate glasses due to the interaction of radiative energy between Er^{3+} ions by strongly overlapping of electron shell with ligand shell in emission and absorption bands [47]. On the other hand, the displacement of energy between Er^{3+} ions also affect the changes of σ_e value [48]. Figure of merit (FOM, FHWM × σ_e) is a key factor for optical amplifier application. The higher its value, the better its performance. The FOM of LiBEr3, LiBEr4, LiBEr5 and LiBEr6 are 349.11, 301.7, 415.25 and 206.58 × 10^{-28} cm^3, respectively. The highest FOM of LiBEr5 is much higher compared to the FOM of other glass such as TCZNEr1 and erbium doped zinc bismuth borate (ZBE3) [49]. The branching ratios (β_R) for all samples are 1 which is consistent to the standard branching ratio with value between 1 and 1.5. The lifetimes of LiBEr3, LiBEr4, LiBEr5 and LiBEr6 are 8.674, 8.919, 7.101, and 13.012 ms, respectively. Compared to the other reports the present data is comparable with Er^{3+} doped several host glasses. The radiative transition probabilities are 115.28, 106.27, 133.25, and 76.85 S^{-1} for LiBEr3, LiBEr4, LiBEr5 and LiBEr6, respectively.

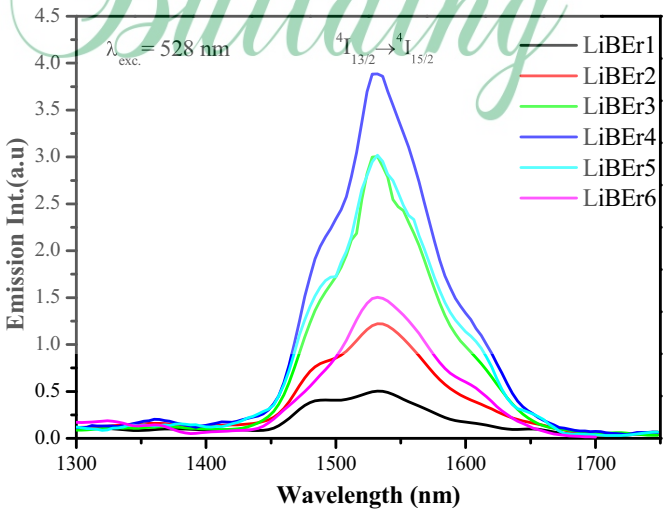

Fig. 6. Near-infrared luminescence spectra of Er^{3+} doped sodium lithium borate glasses system for λ_{exc} = 582 nm.

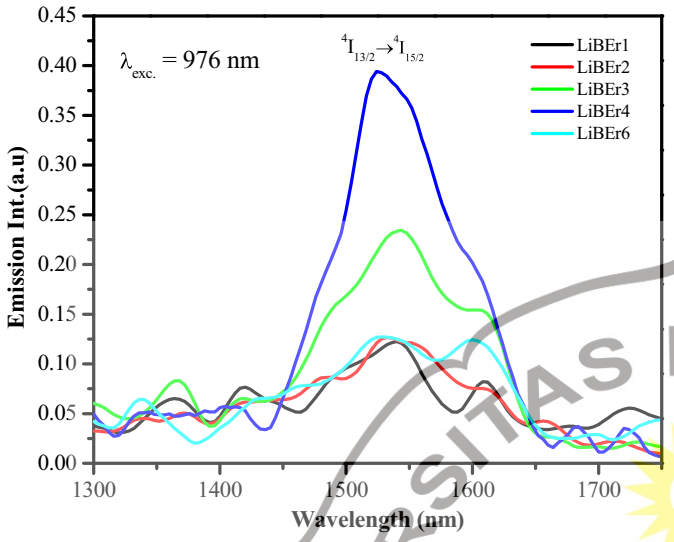

Fig. 7. Near-infrared luminescence spectra of Er^{3+} doped sodium lithium borate glasses system for $\lambda_{exc} = 976$ nm.

4. Conclusion

The Er^{3+} ions doped lithium-borate glasses with chemical composition (65-x)B_2O_3-15Na_2O-10PbO-5ZnO-5Li_2O-xEr_2O_3 had been successfully prepared by the melting-quench method. The XRD analysis showed that all samples were amorphous nature without any crystalline phase. The structural analysis by FTIR confirmed the presence of bending vibration B-O-B in borate networks, B—O bond stretching of tetrahedral BO_4 units, and asymmetric stretching of the B—O vibrations in trigonal BO_3 units. The absorption and luminescence spectra of glass samples were measured to investigate the spectroscopic properties. The absorption band at UV–Vis-NIR located at 365, 380, 407, 451, 489, 521, 543, 652, 797, 974 and 1528 nm correspond to the $^4I_{15/2} \rightarrow {}^2G_{9/2}$, $^4G_{9/2}$, $^4G_{11/2}$, $^2H_{9/2}$, $^4F_{5/2}$, $^4F_{7/2}$, $^2H_{11/2}$, $^4S_{3/2}$, $^4F_{9/2}$, $^4I_{9/2}$, $^4I_{11/2}$ and $^4I_{13/2}$, respectively. The highest absorption is found at band transition from $^4I_{15/2} \rightarrow {}^2H_{11/2}$ and called as a hypersensitive transition. The Judd–Ofelt parameters were Ω_2, = 4.39, Ω_4 = 3.22, and Ω_6 = 0.91 ($\times 10^{-22}$ cm^2) for 2.0 mol% Er^{3+} ion doped sodium lithium borate glass. A strong emission band at 1532 nm was observed corresponding to $^4I_{15/2} \rightarrow {}^4I_{13/2}$ transition under the excitation wavelength of 528 and 976 nm. We found that sample with 2.0 mol% Er^{3+} ion doped sodium lithium borate glass (LiBEr5) had the highest stimulated emission cross-section and were comparable with the previous reports. The Er^{3+} doped sodium lithium borate glass is considered having the great potential for infrared laser and optical amplifier applications.

Acknowledgments

The authors would like to thank Kementerian Riset Teknologi Dan Pendidikan Tinggi Republik Indonesia for financial support of this project.

References

[1] S. Hraiech, N. Sdiri, K. Horchani-Naifer, M. Férid, Thermal and optical properties of Er3+ doped phosphate glasses, J. Non-Cryst. Solids 482 (2018) 73–77, https://doi.org/10.1016/j.jnoncrysol.2017.12.018.
[2] Y.C. Ratnakaram, A.V. Reddy, R.P.S. Chakradhar, Electronic absorption spectra and energy gap studies of Er3+ ions in different chlorophosphate glasses, Spectrochim. Acta A 58 (2002) 1809–1822, https://doi.org/10.1016/S1386-1425(01)00631-X.
[3] J. Rajagukguk, J. Kaewkhao, M. Djamal, R. Hidayat, Y. Ruangtaweep, Structural and optical characteristics of Eu3+ ions in sodium-lead-zinc-lithium-borate glass system, J. Mol. Struct. 1121 (2016) 180–187, https://doi.org/10.1016/j.molstruc.2016.05.048.
[4] J. Rajagukguk, R. Hidayat, M. Djamal, Y. Ruangtaweep, M. Horprathum, J. Kaewkhao, Structural and optical properties of Nd3+ doped Na2O-PbO-ZnO-Li2O-B2O3 glasses system, Key Eng. Mater. vol. 675, 2016, pp. 424–429, https://doi.org/10.4028/www.scientific.net/KEM.675-676.424.
[5] I. Kindrat, B. Padlyak, A. Drzewiecki, Luminescence properties of the Sm-doped borate glasses, J. Lumines. 166 (2015) 264–275, https://doi.org/10.1016/j.jlumin.2015.05.051.
[6] P. Pawar, S. Munishwar, R. Gedam, Intense white light luminescent Dy3+ doped lithium borate glasses for W-LED: a correlation between physical, thermal, structural and optical properties, Solid State Sci. 64 (2017) 41–50, https://doi.org/10.1016/j.solidstatesciences.2016.12.009.
[7] L.R. Moorthy, T.S. Rao, K. Janardhnam, A. Radhapathy, Absorption and emission characteristics of Er3+ ions in alkali chloroborophosphate glasses, Spectrochim. Acta A 56 (2000) 1759–1771, https://doi.org/10.1016/S1386-1425(00)00234-1.
[8] H. Lin, G. Meredith, S. Jiang, X. Peng, T. Luo, N. Peyghambarian, E.Y.-B. Pun, Optical transitions and visible upconversion in Er3+ doped niobic tellurite glass, J. Appl. Phys. 93 (2003) 186–191, https://doi.org/10.1063/1.1527209.
[9] Y. Hao, J. Cao, Structure and luminescence of Dy3+ doped CaO–B2O3–SiO2 glasses, Physica B Condens Matter 493 (2016) 68–71, https://doi.org/10.1016/j.physb.2016.04.017.
[10] C. Kam, S. Buddhudu, Emission analysis of Eu3+: Bi2O3–B2O3–R2O (R= Li, Na, K) glasses, J. Quant. Spectrosc. Radiat. Transf. 87 (2004) 325–337, https://doi.org/10.1016/j.jqsrt.2004.03.006.
[11] R. Gopalakrishnan, N. Rajeshwari, S. Buddhudu, Optical-physical-electrical properties of Er3+: B2O3-BaO-RF glasses, J. Alloys Compd. 275 (1998) 327–332, https://doi.org/10.1016/S0925-8388(98)00333-8.
[12] A.S. Rao, J.L. Rao, R.R. Reddy, T.R. Rao, Electron paramagnetic resonance and optical absorption spectra of Cr (III) ions in alkali cadmium borosulphate glasses, Opt. Mater. 4 (1995) 717–721, https://doi.org/10.1016/0038-1098(95)00375-4.
[13] V. Uma, K. Marimuthu, G. Muralidharan, Effect of modifier oxides (SrO, Al2O3, ZnO, CdO, PbO and Bi2O3) on the luminescence properties of Er3+ doped telluroborate glasses for laser and optical amplifier applications, J. Lumines. 207 (2019) 534–544, https://doi.org/10.1016/j.jlumin.2018.12.001.
[14] A.M. Abdelghany, H.A. ElBatal, F.M. EzzElDin, Bone bonding ability behavior of some ternary borate glasses by immersion in sodium phosphate solution, Ceram. Int. 38 (2012) 1105–1113, https://doi.org/10.1016/j.ceramint.2011.08.038.
[15] K. Annapoorani, C. Basavapoornima, N. Suriya Murthy, K. Marimuthu, Investigations on structural and luminescence behavior of Er3+ doped Lithium zinc borate glasses for lasers and optical amplifier applications, J. Non-Cryst. Solids 447 (2016) 273–282, https://doi.org/10.1016/j.jnoncrysol.2016.06.021.
[16] H. Fan, G. Wang, K. Li, L. Hu, Broadband 1.5-μm emission of high erbium-doped Bi2O3–B2O3–Ga2O3 glasses, Solid State Commun. 150 (2010) 1101–1103, https://doi.org/10.1016/j.ssc.2010.03.031.
[17] A. Thulasiramudu, S. Buddhudu, Optical characterization of Sm3+ and Dy3+: ZnO–PbO–B2O3 glasses, Spectrochim. Acta A 67 (2007) 802–807, https://doi.org/10.1016/j.saa.2006.08.036.
[18] P. Pawar, S. Munishwar, S. Gautam, R. Gedam, Physical, thermal, structural and optical properties of Dy3+ doped lithium alumino-borate glasses for bright W-LED, J. Lumines. 183 (2017) 79–88, https://doi.org/10.1016/j.jlumin.2016.11.027.

Table 5
Radiative properties, such as emission peak wavelength (λ_p), effective bandwidth ($\Delta\lambda_{eff}$), emission cross-section ($\sigma_e(\lambda_p) \times 10^{-21}$), FOM (($FWHM \times \sigma_e) \times 10^{-28}$), branching ratio ($\beta_R$), lifetime ($\tau_R$), and radiative transition probability (A_R) of various Er^{3+}-doped sodium borate glasses for the $^4I_{13/2} \rightarrow {}^4I_{15/2}$ transition.

Samples	λ_p (nm)	$\Delta\lambda_{eff}$ (nm)	FWHM (nm)	σ_e (λ_p) (cm^2)	FOM (cm^3)	β_R (%)	τ_R (ms)	A_R (s^{-1})	Ref.
LiBEr3	1532	91.12	97.79	3.57	349.11	1	8.674	115.28	This work
LiBEr4	1532	98.36	98.92	3.05	301.71	1	8.919	106.27	This work
LiBEr5	1532	100.26	104.86	3.96	415.25	1	7.101	133.25	This work
LiBEr6	1532	100.34	95.64	2.16	206.58	1	13.01	76.85	This work
Er^{3+}-2PbO·4ZnO·5B_2O_3	1531	87.4	–	0.7	–	0.3	–	16.6	[41]
TCZNBEr1	1529	80.82	81	3.22	260.82	1	4.36	–	[46]
ZBE3	1510	70	70	3.84	268.8	0.2			[49]

[19] Y. Chen, Y. Huang, M. Huang, R. Chen, Z. Luo, Spectroscopic properties of Er3+ ions in bismuth borate glasses, Opt. Mater. 25 (2004) 271–278, https://doi.org/10.1016/j.optmat.2003.07.002.
[20] A.M. Ibrahim, A.H. Hammad, A.M. Abdelghany, G.O. Rabie, Mixed alkali effect and samarium ions effectiveness on the structural, optical and non-linear optical properties of borate glass, J. Non-Cryst. Solids 495 (2018) 67–74, https://doi.org/10.1016/j.jnoncrysol.2018.05.015.
[21] F.H. El Batal, A.A. El Kheshen, M.A. Azooz, S.M. Abo-Naf, Gamma ray interaction with lithium diborate glasses containing transition metals ions, Opt. Mater. 30 (2008) 881–891, https://doi.org/10.1016/j.optmat.2007.03.010.
[22] A.M. Abdelghany, H.A. ElBatal, Optical and μ-FTIR mapping: a new approach for structural evaluation of V2O5-lithium fluoroborate glasses, Mater. Des. 89 (2016) 568–572, https://doi.org/10.1016/j.matdes.2015.09.159.
[23] K. Mariselvam, R.A. Kumar, K. Suresh, Optical properties of Nd3+ doped barium lithium fluoroborate glasses for near-infrared (NIR) emission, Physica B 534 (2018) 68–75, https://doi.org/10.1016/j.physb.2017.12.064.
[24] C. Basavapoornima, K. Linganna, C.R. Kesavulu, S. Ju, B.H. Kim, W.T. Han, C.K. Jayasankar, Spectroscopic and pump power dependent upconversion studies of Er3+−doped lead phosphate glasses for photonic applications, J. Alloy. Compd. 699 (2017) 959–968, https://doi.org/10.1016/j.jallcom.2016.12.199.
[25] K. Selvaraju, K. Marimuthu, Structural and spectroscopic studies on Er3+ doped boro-tellurite glasses, Physica B 407 (2012) 1086–1093, https://doi.org/10.1016/j.physb.2012.01.003.
[26] R.F. de Morais, E.O. Serqueira, N.O. Dantas, Effect of thermal annealing on the spectroscopic parameters of Er3+−doped sodium silicate glass, Opt. Mater. 35 (2013) 2122–2127, https://doi.org/10.1016/j.optmat.2013.05.032.
[27] S. Babu, M. Seshadri, V.R. Prasad, Y. Ratnakaram, Spectroscopic and laser properties of Er3+ doped fluoro-phosphate glasses as promising candidates for broadband optical fiber lasers and amplifiers, Mater. Res. Bull. 70 (2015) 935–944, https://doi.org/10.1016/j.materresbull.2015.06.033.
[28] T. Rao, A.R. Kumar, K. Neeraja, N. Veeraiah, M.R. Reddy, Optical and structural investigation of Eu3+ ions in Nd3+ co-doped magnesium lead borosilicate glasses, J. Alloys Compd. 557 (2013) 209–217, https://doi.org/10.1016/j.jallcom.2012.12.162.
[29] C. Kesavulu, H. Kim, S. Lee, J. Kaewkhao, N. Wantana, S. Kothan, S. Kaewjaeng, Influence of Er3+ ion concentration on optical and photoluminescence properties of Er3+−doped gadolinium-calcium silica borate glasses, J. Alloys Compd. 683 (2016) 590–598, https://doi.org/10.1016/j.jallcom.2016.04.314.
[30] A.R. Devi, C. Jayasankar, Optical properties of Er3+ ions in lithium borate glasses and comparative energy level analyses of Er3+ ions in various glasses, J. Non-Cryst. Solids 197 (1996) 111–128, https://doi.org/10.1016/0022-3093(95)00573-0.
[31] Q. Chen, M. Ferraris, Y. Menke, D. Milanese, E. Monchiero, Novel erbium doped PbO and B2O3 based glasses with broad 1.5 μm absorption line width and low refractive index, J. Non-Cryst. Solids 324 (2003) 1–11, https://doi.org/10.1016/S0022-3093(03)00222-9.
[32] I.A. Rayappan, K. Marimuthu, Structural and luminescence behavior of the Er3+ doped alkali fluoroborate glasses, J. Non-Cryst. Solids 367 (2013) 43–50, https://doi.org/10.1016/j.jnoncrysol.2013.02.016.
[33] N. Vijaya, P. Babu, V. Venkatramu, C. Jayasankar, S. León-Luis, U. Rodríguez-Mendoza, I. Martín, V. Lavín, Optical characterization of Er3+−doped zinc fluorophosphate glasses for optical temperature sensors, Sens. Actuators B Chem. 186 (2013) 156–164, https://doi.org/10.1016/j.snb.2013.05.081.
[34] S.F. León-Luis, U.R. Rodríguez-Mendoza, P. Haro-González, I.R. Martín, V. Lavín, Role of the host matrix on the thermal sensitivity of Er3+ luminescence in optical temperature sensors, Sens. Actuators B Chem. 174 (2012) 176–186, https://doi.org/10.1016/j.snb.2012.08.019.
[35] S. Liu, G. Zhao, Y. Li, H. Ying, J. Wang, G. Han, Optical absorption and emission properties of Er3+ doped mixed alkali borosilicate glasses, Opt. Mater. 30 (2008) 1393–1398, https://doi.org/10.1016/j.optmat.2007.08.002.
[36] K. Binnemans, R. Van Deun, C. Görller-Walrand, J.L. Adam, Optical properties of Nd3+−doped fluorophosphate glasses, J. Alloy. Compd. 275-277 (1998) 455–460, https://doi.org/10.1016/S0925-8388(98)00367-3.
[37] S. Dai, W. Xiang, T. Xu, Q. Nie, X. Shen, Effect of radiation trapping on the emission properties of Er3+: 4I13/2→4I15/2 transition in oxide glasses, Opt. Mater. 30 (2008) 1355–1360, https://doi.org/10.1016/j.optmat.2007.06.014.
[38] Q. Qian, Y. Wang, Q. Zhang, G. Yang, Z. Yang, Z. Jiang, Spectroscopic properties of Er3+−doped Na2O–Sb2O3–B2O3–SiO2 glasses, J. Non-Cryst. Solids 354 (2008) 1981–1985, https://doi.org/10.1016/j.jnoncrysol.2007.11.005.
[39] A. Awang, S. Ghoshal, M. Sahar, R. Arifin, Gold nanoparticles assisted structural and spectroscopic modification in Er3+−doped zinc sodium tellurite glass, Opt. Mater. 42 (2015) 495–505, https://doi.org/10.1016/j.optmat.2015.02.009.
[40] K. Swapna, S. Mahamuda, M. Venkateswarlu, A.S. Rao, M. Jayasimhadri, S. Shakya, G.V. Prakash, Visible, up-conversion and NIR (similar to 1.5 mu m) luminescence studies of Er3+ doped zinc Alumino bismuth borate glasses, J. Lumines. 163 (2015) 55–63, https://doi.org/10.1016/j.jlumin.2015.02.036.
[41] A. Speghini, M. Peruffo, M. Casarin, D. Ajò, M. Bettinelli, Electronic spectroscopy of trivalent lanthanide ions in lead zinc borate glasses, J. Alloy. Compd. 300-301 (2000) 174–179, https://doi.org/10.1016/S0925-8388(99)00718-5.
[42] K. Pradeesh, C. Oton, V. Agotiya, M. Raghavendra, G.V. Prakash, Optical properties of Er3+ doped alkali chlorophosphate glasses for optical amplifiers, Opt. Mater. 31 (2008) 155–160, https://doi.org/10.1016/j.optmat.2008.02.007.
[43] S. Xu, Z. Yang, S. Dai, J. Yang, L. Hu, Z. Jiang, Spectral properties and thermal stability of Er3+−doped oxyfluoride silicate glasses for broadband optical amplifier, J. Alloy. Compd. 361 (2003) 313–319, https://doi.org/10.1016/S0925-8388(03)00447-X.
[44] M.J. Weber, Probabilities for radiative and nonradiative decay of Er^{3+} in LaF_3, Phys. Rev. 157 (1967) 262–272, https://doi.org/10.1103/PhysRev.157.262.
[45] S. Kang, X. Wang, W. Xu, X. Wang, D. He, L. Hu, Effect of B2O3 content on structure and spectroscopic properties of neodymium-doped calcium aluminate glasses, Opt. Mater. 66 (2017) 287–292, https://doi.org/10.1016/j.optmat.2017.02.021.
[46] O. Ravi, S.J. Dhoble, B. Ramesh, G. Devarajulu, C.M. Reddy, K. Linganna, G.R. Reddy, B.D.P. Raju, NIR fluorescence spectroscopic investigations of Er3+−ions doped borate based tellurium calcium zinc niobium oxide glasses, J. Lumines. 164 (2015) 154–159, https://doi.org/10.1016/j.jlumin.2015.03.040.
[47] Y. Guan, Z. Wei, Y. Huang, R. Maalej, H.J. Seo, 1.55μm emission and upconversion luminescence of Er3+ doped strontium borate glasses, Ceram. Int. 39 (2013) 7023–7027, https://doi.org/10.1016/j.ceramint.2013.02.040.
[48] V. Lavín, I. Martin, U. Rodríguez-Mendoza, V. Rodríguez, Energy transfer between Eu3+ ions in calcium diborate glasses, J. Phys. Condens. Matter 11 (1999) 8739, https://doi.org/10.1088/0953-8984/11/44/312.
[49] I. Pal, S. Sanghi, A. Agarwal, M.P. Aggarwal, Spectroscopic and structural investigations of Er3+ doped zinc bismuth borate glasses, Mater. Chem. Phys. 133 (2012) 151–158, https://doi.org/10.1016/j.matchemphys.2011.12.086.